ADVANCED MATERIALS
www.advmat.de

Contributions of Different Functional Groups to Contact Electrification of Polymers

Shuyao Li, Jinhui Nie, Yuxiang Shi, Xinglin Tao, Fan Wang, Jingwen Tian, Shiquan Lin, Xiangyu Chen, and Zhong Lin Wang**

Polymers are commonly used to fabricate triboelectric nanogenerators (TENGs). Here, several polymer films with similar main chains but different functional groups on the side chain are employed to clarify the contributions of each functional group to contact electrification (CE). The results show that the electron-withdrawing (EW) ability and density of these functional groups on the main chain can determine both the polarity and density of CE-induced surface charges. Similar results are obtained for CE in both the polymer–polymer and polymer–liquid modes. A theoretical mechanism involving electron cloud overlap is proposed to explain all of these results. More importantly, the unsaturated groups on poly(tetrafluoroethylene) molecular chain are proved to have a much stronger EW ability than the saturated groups. The density of these unsaturated groups can be increased using a sputtering technique, suggesting that this is a facile and effective method of enhancing the performance of TENGs. These results clarify the correlation between the molecular structure and macroscopic electrification behavior of polymers.

Contact electrification (CE) is a common phenomenon in everyday life and has been known for more than 2600 years. However, the mechanism of CE and the physical origin of the CE-induced surface charges have long been a subject of heated debate, especially for CE involving liquid materials.[1–5] Since 2012, the rapid development of triboelectric nanogenerators (TENGs),[6–9] which exploit the CE effect to harvest various types of mechanical energy, has strongly motivated the fundamental study of CE.[9–15] Various recent experimental findings, such as the thermionic emission effect[16] and photon excitation effect of CE-induced charges,[17] have confirmed that electron transfer due to overlapping electron clouds dominates the CE between solids and solids, and even, in some cases, that between solids and liquids, which is called the Wang transition.[18–20] In addition, the output of TENGs has been increasing continuously. Quite recently, Wang et al. found that the CE between a tiny droplet and a poly(tetrafluoroethylene) (PTFE) film can light 100 light-emitting diodes;[3] this result has also inspired many researchers to further consider the underlying mechanism of charge generation at the liquid–solid interface. However, even though the dominant role of electron transfer in CE has been confirmed, the electron transfer between different triboelectric materials (solid or liquid) at the molecular level has still not been studied in sufficient detail.

In addition, most of the triboelectric materials used in TENGs are polymer-based, mainly owing to the flexibility, smoothness, and strong electrification ability of polymers,[21–23] and considerable evidence suggests that the characteristics of the functional groups and chemical structure of the polymer can determine the CE performance.[24–27] For example, by attaching different functional groups to the surface of the polymer, researchers can not only enhance the charge density but also change its polarity during CE.[28,29] In addition, modifying the phase composition of a poly(vinylidene difluoride) (PVDF) copolymer increases the net dipole moment, which results in a significant increase in the CE-induced surface charge density.[30,31] A recent study has also confirmed that the radiation-induced damage to chemical bonds can increase the electron-donating (ED) ability of polyimide during CE.[32] Hence, systematic study of the underlying relationships between different functional groups and the CE effect based on the latest electron transfer model is essential for better understanding the physical mechanism of TENGs.

For this study, we selected a series of polymer films with similar carbon chains but different functional groups on the side chain and studied the CE performance in both solid and liquid materials. Among the functional groups, the fluorine groups on the C chain show the strongest electron-withdrawing (EW) ability, and the fluorinated ethylene propylene (FEP) film,

S. Li, J. Nie, Y. Shi, X. Tao, F. Wang, J. Tian, Dr. S. Lin, Prof. X. Chen, Prof. Z. L. Wang
CAS Center for Excellence in Nanoscience
Beijing Key Laboratory of Micro-nano Energy and Sensor
Beijing Institute of Nanoenergy and Nanosystems
Chinese Academy of Sciences
Beijing 100083, P. R. China
E-mail: chenxiangyu@binn.cas.cn

S. Li, J. Nie, X. Tao, F. Wang, J. Tian, Dr. S. Lin, Prof. X. Chen, Prof. Z. L. Wang
School of Nanoscience and Technology
University of Chinese Academy of Sciences
Beijing 100049, P. R. China

Prof. Z. L. Wang
School of Material Science and Engineering
Georgia Institute of Technology
Atlanta, GA 30332-0245, USA
E-mail: zhong.wang@mse.gatech.edu

The ORCID identification number(s) for the author(s) of this article can be found under https://doi.org/10.1002/adma.202001307.

DOI: 10.1002/adma.202001307

which contains the $-CF_3$ group, exhibits the highest charge density. The CE effects in the polymer–polymer and polymer–liquid modes were similar. More importantly, the CE contribution of the unsaturated groups on the PTFE molecular chain was revealed for the first time. These unsaturated groups have a very strong EW ability, which is much stronger than that of the common ($-CF_2-CF_2-$) group on the main chain. The density of these unsaturated groups can be increased by sputtering a very thin film of PTFE on the original PTFE film surface. These studies illuminate the correlation between the molecular structure and macroscopic electrification behavior of materials.

The experimental system for studying the CE in the polymer–solid and polymer–liquid modes is shown in **Figure 1**a,b. Polymers with similar main chains but different side-chain functional groups are used as solid materials, and the CE-induced charges on their surface are measured to determine the electrification ability. In the polymer–solid mode (Figure 1a), a vertical contact-separation TENG is employed, and the triboelectric response of the polymers is indicated by the amount of charge transfer between the polymer and metal. In the polymer–liquid mode (Figure 1b), a certain number of deionized water droplets is pressed between two polymer films, and the CE-induced charges on the water droplet are measured after separation, as described in a previous work. Polymers with a carbon main chain and different functional groups are selected, specifically, a polypropylene (PP) film (methyl group), a poly(vinyl alcohol) (PVA) film (alcohol group), a poly(vinyl chloride) (PVC) film (chlorine group), a polyethylene (PE) film (hydrogen group), a PVDF film (bifluoride group), a PTFE film (tetrafluoro group), and an FEP film (trifluoromethyl group) (Figure 1c). The thickness of these films is fixed at 50 µm, and the roughness is ±50 nm, as shown in Figures S1 and S2 in the Supporting

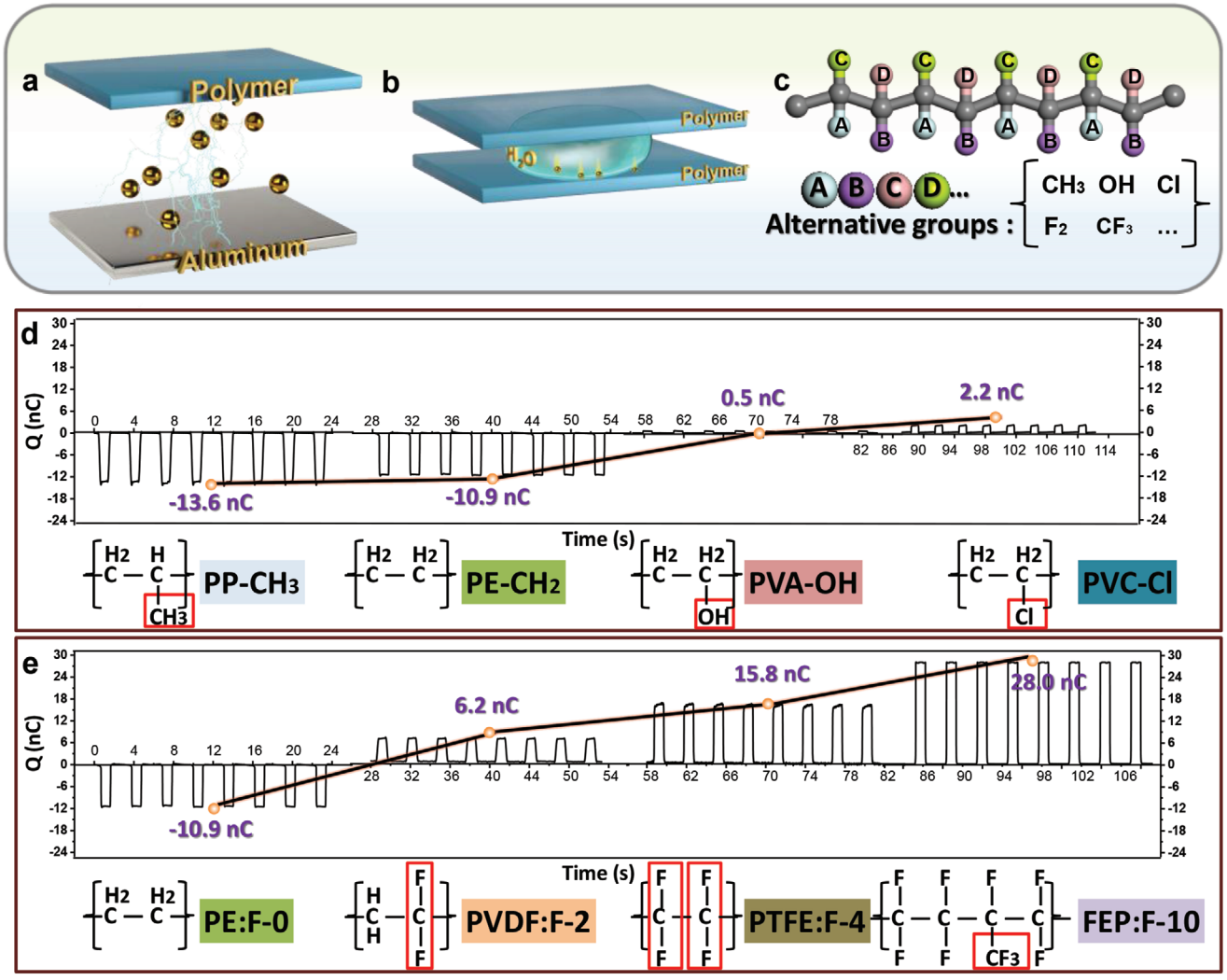

Figure 1. a) A vertical contact-separation TENG has been employed for the measurements and the contact area are all kept to be 40 mm × 40 mm. b) TENG for testing the polymer–liquid CE and the drop volume is 50 µL. c) Alternative polymer films have carbon as the main chain and A/B/C/D as the side chain. d) Polymer films of PP, PE, PVA, and PVC are contacted with Al foil to show their electrification ability. The electrode underneath polymer films are connected to the red wire of the electrometer; PE/PP films are positive and PVA/PVC films are negative. The amounts of transferred charges (Q) are recorded. e) The amount of Q between the F-containing polymers and Al, which are PE film-without F, PVDF film-bifluoro, PTFE film-tetrafluoro and FEP film-polyfluoro. PE film is positively charged and the other films are negatively charged.

Information. The effective contact area of the TENG in Figure 1 is 40 mm × 40 mm, and an aluminum foil is selected as the reference tribomaterial in contact with the polymers. The scanning microscopy (SEM) image of the Al film in Figure S3 in the Supporting Information shows that the Al surface is rather smooth, with a roughness within ±25 nm. The surface roughness of the Al film is low enough that the roughness has little effect on the CE; thus, the contributions of the functional groups are more apparent. In the polymer–solid mode, each polymer, which acts as one of the tribomaterials in a contact-separation TENG, is attached on top of a metal electrode, and the Al foil is attached to the other side. Both the metal electrode and the Al foil are connected to a Keithley 6514 electrometer. Figure 1d clearly shows that the PP and PE films are positively charged after contacting the Al, and the charge transfer is −13.6 and −10.9 nC, respectively. During CE, the PP and PE films tend to lose electrons when they are in contact with the Al. The methyl group has a greater ED ability than the hydrogen group; thus, the PP film appears to be more positive than the PE film. The PVA and PVC films show negative charges, and the PVC film (2.2 nC) is more negative than the PVA film (0.5 nC) because the chlorine group is a stronger EW group, which tends to attract more electrons than the alcohol group. When the main chain is the same, the different groups on the side chain determine the polarity of the polymer in CE. However, for polymers with the same main chain and side groups, the electrification can also be affected by the density of the side-chain groups. As shown in Figure 1e, as the number of F groups on the side chain increases, the charge transfer also increases. During CE with Al, the charge transfer amounts of the PE film (without F), PVDF film (bifluoride group), PTFE film (tetrafluoride group), and FEP film (polyfluoride group) in the polymerization unit are −10.9, 6.2, 15.8, and 28.0 nC, respectively. Hence, the presence of strong EW groups such as F groups on the side chain results in the generation of negative charges on the polymer surface during CE. Note that the roughness of the films may slightly affect the size of the effective contact area, but we believe that this effect may be very small, because these polymers have comparable surface roughness values (Figure S1, Supporting Information). We also measured the microscale tribo-induced potential change on these polymers during CE with the metal probe using atomic force microscopy,[33,34] which may clarify the possible effect of the surface roughness. The results were in good agreements with the results from the TENGs. The glass transition temperatures of the polymers are −10 °C for the PP film, 20 °C for the PVA film, 87 °C for the PVC film, −68 °C for the PE film, −35 °C for the PVDF film, and −55 °C for the FEP film. Thus, these materials are in a rubbery state at room temperature. In addition, the Young's moduli of these materials are ≈1.5 ± 0.9 GPa, except for that of the PVA film, which is 13 GPa, as shown in Table S1.

To further clarify the relationship between the functional groups and the CE effect, four polymers with different F group densities on the C chain (Figure S2d–g, Supporting Information) are brought into contact with each other, and the induced charge transfer is recorded (**Figure 2**a). The experimental setup for this test is based on a common contact-separation TENG with double dielectric layers.[35] A PE film connected to the red wire of the electrometer is placed in contact with the PVDF, PTFE, or FEP film; the measured charge transfer is 9.7, 13.7, and 66.2 nC, respectively (Figure 2b–d). The output current (Figure S4a—c, Supporting Information) reveals that the PE film is more positively charged during CE than the other three films, indicating that its F groups give it a stronger EW ability. The charge transfer results and the output current of the TENGs consisting of PVDF–PTFE, PVDF–FEP, and PTFE–FEP are shown in Figure S4d–f in the Supporting Information, and the charge transfer in these three devices is 6.2, 63.4, and 41.1 nC, respectively. Interestingly, the EW ability of the polymers increases with increasing density of the F groups on the side chain (Figure 2e–g). Thus, the FEP film, which contains the $-CF_3$ group, always captures more electrons during CE with the other polymers. The results of a similar experiment using the other polymers (PP, PE, PVA, and PVC) are shown in Figure S5 in the Supporting Information. The strength of the EW ability of each functional group follows the order $CH_3 < H < OH < Cl < F$.

On the other hand, the CE results obtained in the polymer–liquid mode (Figures 1a and 2h–k) were also studied, and the amount of tribo-induced charge on the water droplets is measured using an electric meter.[22] The volume of the deionized water is fixed at 50 µL. In this polymer–liquid mode, the deionized water is always positively charged, and the use of contact under pressure can maximize the contact area between the droplet and polymer film, which in turn can maximize the CE charges generated on the droplet.[22] PVA is soluble in water; thus, no solid–liquid electrification tests were performed, and only the other six films were tested using this experimental setup. Recent work has demonstrated that the CE between a fluoropolymer and an aqueous solution varies with the contact angle.[36] The average contact angles of water on the six films are 98° for the PP film, 84° for the PVC film, 97° for the PE film, 97° for the PVDF film, 98° for the PTFE film, and 94° for the FEP film (Figure S6, Supporting Information). These contact angles are comparable, except for that of the PVC film. The electrification ability of PVC in the polymer–liquid mode (Figure 2h–k) is very low. To explain this phenomenon, we need to consider the ion adsorption effect. Positive ions (H^+) may have adhered to the PVC surface during CE with water and limited the electron transfer. A similar phenomenon was observed in our previous study on a MgO surface,[23] where both electrons and hydrogen ions were attracted to the surface of a MgO film, and a neutralization effect was identified. Note that the PE and PP films appear to be positively charged when they are in contact with Al, but they are negatively charged when they are in contact with water. When the contact area of the PP film and water increases from 0.5 to 4.0 cm^2 (under pressure in the vertical direction), the CE charge changes from 0.5 to 0.6 nC (Figure 2h–k). The CE charges of the PE and PVDF films increase by 33% (0.6–0.8 nC) and 43% (0.7–1.0 nC), respectively. The CE between a polymer and a liquid is believed to be dominated by either hydroxide adsorption or electron transfer.[22,23] The functional groups in the PE and PP films have been demonstrated to have very weak EW ability, suggesting that it is difficult for them to capture electrons during contact with water droplets. Thus, the adsorption effect of hydroxide ions could be the main reason for the negatively charged surface after CE. According to our previous study, the increase in contact area

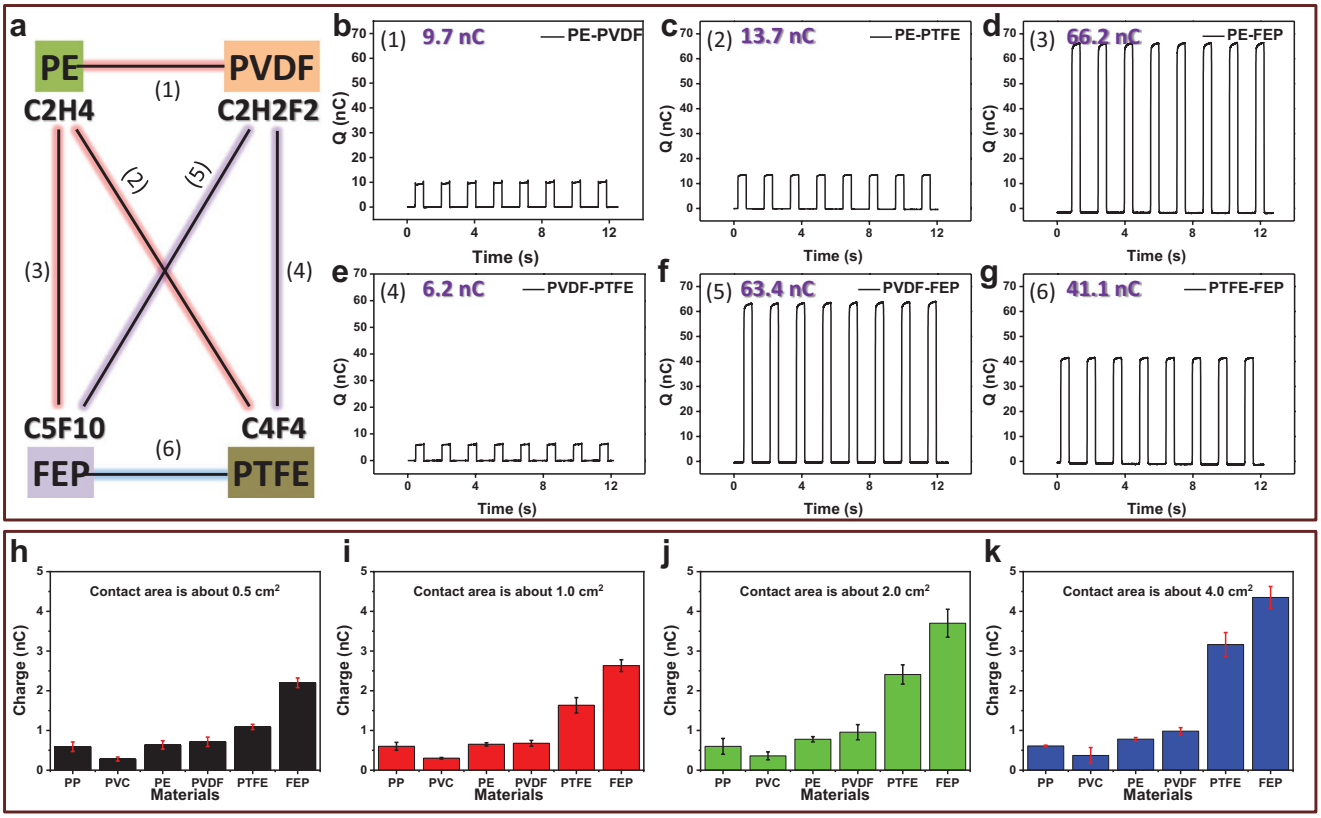

Figure 2. a) The schematic diagram of CE among the four selected polymer films in the polymer–polymer mode. PE film in line (1), (2), (3), PVDF film in line (4), (5), and PTFE film in line (6) are connected to the red line of the electrometer. b) The charge transfer (Q) for PE-PVDF TENG device and PE film is positive; c) The Q for PE-PTFE TENG device and PE film is positive; d) The Q for PE-FEP TENG device and PE film is positive; e) The Q for PVDF-PTFE TENG device and PVDF film is positive; f) The Q for PVDF-FEP TENG device and PVDF film is positive; g) The Q for PTFE-FEP TENG device and PTFE film is positive; the contact areas are all kept to be 40 mm × 40 mm. h–k) In the polymer–liquid mode, the Q for the four selected films after contacting with the water: the maximum contact area is about: h) 0.5 cm^2, i) 1.0 cm^2, j) 2.0 cm^2, k) 4.0 cm^2; the volume of water is 50 µL. Water is always positively charged.

results in a significant increase in the tribo-induced charge on the droplet,[22] which is a typical result for the electron transfer model of CE. However, if the ion transfer effect dominates the CE at a liquid–solid interface, increasing the contact area may not increase the tribo-induced charge. Many researchers believe, on the basis of the ion adsorption model, that the concentration of hydroxide ions accumulated on the surface of the water may exceed their bulk concentration,[37–39] which enhances the hydroxide adsorption during the CE at the liquid–solid interface. In this case, the further pressing of the droplets between two polymer films (which squeezes the water from the bulk to the surface) may increase the concentration of hydrogen ions at the surface and thus suppress the preferential adsorption of hydroxide ions. However, there is no effective method of verifying whether ion adsorption actually dominates the CE between PE or PP and water droplets. The amount of ion adsorption on these polymer surfaces is too low to be detected by infrared spectroscopy, Raman spectroscopy, or nuclear magnetic resonance.[22] The experimental error during the measurement should be considered. The electrification performance of these polymers (PP, PVC, and PE) is very weak; thus, the contribution of the interference parameters becomes notable. Even though we carefully reduced the effects of the experimental conditions, the results for PP, PVC, and PE still have large error bars, as shown in Figure 2. By contrast, for PTFE and FEP, a very significant increase in tribo-induced charges with increasing contact area is observed. When the contact area increases from ≈0.5–4.0 cm^2, the CE charge changes from 1.2 to 3.2 nC for the PTFE film and from 2.1 to 4.3 nC for the FEP film, as shown in Figure 2k,h, respectively. Although the rate of increase for FEP (105%) is lower than that for PTFE (166%), the charge on the FEP surface is much larger than that on the PTFE surface. The smaller increase for FEP with increasing contact area may be due to the effect of charge saturation on the droplet.[40] Hence, the strength of the EW ability of the molecular chain can determine the electron transfer process during CE; this finding applies to CE in both the polymer–polymer and polymer–liquid modes, because electron transfer is inevitable during the interaction at the liquid–solid interface. When the volume of the droplets is increased to 100 µL, the CE charge in the solid–liquid mode exhibits similar behavior (Figure S7, Supporting Information). The CE charge from a larger droplet with the same contact area is almost the same as the results in Figure 2h–k, which indicates that the contact area rather than the volume of the droplet is the key factor for CE. Scanning Kelvin probe microscopy was also used to verify the homogeneity

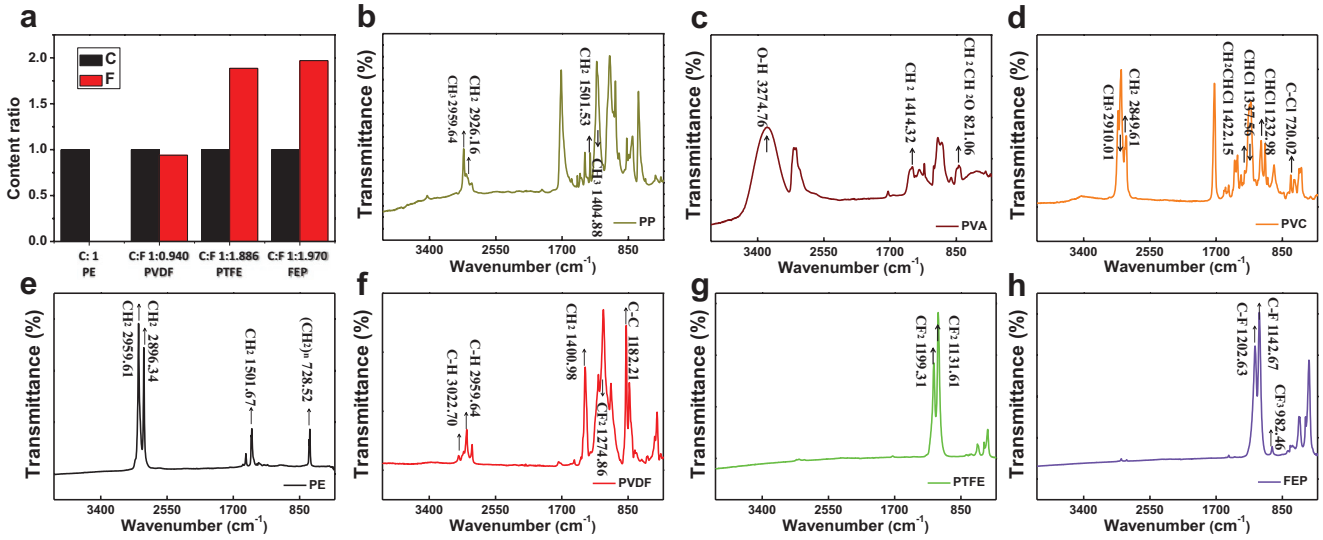

Figure 3. a) The energy-dispersive X-ray spectroscopy (EDX) of C/F ratios of four films: the PE, PVDF, PTFE, FEP films. b–g) The structures of PP film (b), PVA film (c), PVC film (d), PE film (e), PVDF film (f), PTFE film (g), and FEP film (h) are given by a Fourier transform infrared (ATR-FTIR) spectrum and selected polymers are scanned from 4000 to 500 cm^{-1}.

of the charge distribution at the microlevel, as shown in Figure S8a–c in the Supporting Information. Here, the difference in the electrical potential on the PTFE surface before and after contact with the liquid was probed, although we could not observe any mosaic effect. A very small fluctuation of the potential (≈0.2–0.3 V) on the surface is observed, which is within 10% of the total change in the potential.

Selected polymers are analyzed by energy-dispersive X-ray spectroscopy (EDX) and attenuated total reflectance Fourier transform infrared (ATR-FTIR) spectroscopy, and the results are summarized in **Figure 3**. As shown in Figure 3a, the C/F ratios of the PE and FEP films are 1:0 and 1:1.886, respectively, and the F content of the four fluorine-containing films increases gradually. This result can support the conclusion that the charge transfer amount is affected by the presence of F. The ATR-FTIR spectra (Figure 3b–h) and XPS data (Figure S9, Supporting Information) together reveal the molecular structure. Each film clearly has characteristic peaks that reflect the positions of the main chain structure and side-chain groups. According to the XPS analysis (Figure S9a—c, Supporting Information), all three films have a structure based on C—O bonds, which is due to the residue of the initiator used to fabricate the films. The residue may be present only in the chain-end structure but not in the polymerized units, in which case it cannot affect the structure of the polymer itself. Structural analysis reveals that the presence of CH_3 bonds in PP, OH bonds in PVA, and Cl bonds in PVC is reflected in the triboelectric behavior of the films. PP easily loses electrons, and PVC easily gains electrons. The ATR-FTIR spectra show that the F content of the PE, PVDF, PTFE, and FEP films increases gradually from none to F_2/F_3, which proves that the main difference between these films is the F content (Figure 3e–h). According to the XPS spectra, if we ignore the C—C single bonds in the main chain (Figure S9d,e, Supporting Information), C—H bonds occupy the largest area of the PE film, whereas large areas of the PVDF film are occupied by C—F bonds or C—H bonds. In addition, the CF/CF_2 ratio of the PVDF film is 2.98:1, which indicates that the C—F bond plays a dominant role in CE. Similarly, the proportion of CF_2 bonds in PTFE is larger (Figure S9f, Supporting Information), and the area of CF_3 bonds in FEP is the largest (Figure S9g, Supporting Information). Moreover, the CF_2/CF_3 ratios of PTFE and FEP are 7.68:1 and 1:2.40, respectively, indicating that CF_2 is the main EW group in PTFE, and CF_3 is the main EW group in FEP. The CF_2 and CF_3 functional groups both have strong EW ability, although that of CF_3 is slightly stronger than that of CF_2. Thus, the FEP film can induce a stronger tribo-charge than the PTFE film for a small contact area (Figure 2h). The PVDF film contains C—F bonds, and it is unclear which functional groups are exposed to water on the film surface. Consequently, the PVDF film exhibits poor electrification performance compared with the PTFE and FEP films. The XPS results are consistent with the ATR-FTIR spectra, indicating that electron transfer during the CE in both the polymer–polymer and polymer–liquid modes can be explained well in terms of the structure of the functional groups. In addition, for the CE in the polymer–liquid mode, if the functional groups do not have strong ED or EW ability, electron transfer may be suppressed, and we may need to reconsider the contribution of the ion adsorption effect.

The electron transfer is the key element of CE with both polymer–polymer mode and polymer–liquid mode.[34] The core concept of this electron transfer model is related to the motion of electrons outside atomic nuclei during the overlapping of the electron clouds. With the consideration of the EW ability of functional group, we proposed a theoretical mechanism to explain the electron transfer principle between polymer–polymer and between polymer–liquid, as shown in **Figure 4**. In this simplified mechanism mode, the electron cloud indicates the chance of an electron appearing outside the nucleus. When the atomic nuclei have weak EW ability, the electron cloud can occupy a large range. On the contrary, when atomic nuclei have strong EW ability, the atom is covered with a small electron cloud. The shorter molecular chain is used to represent

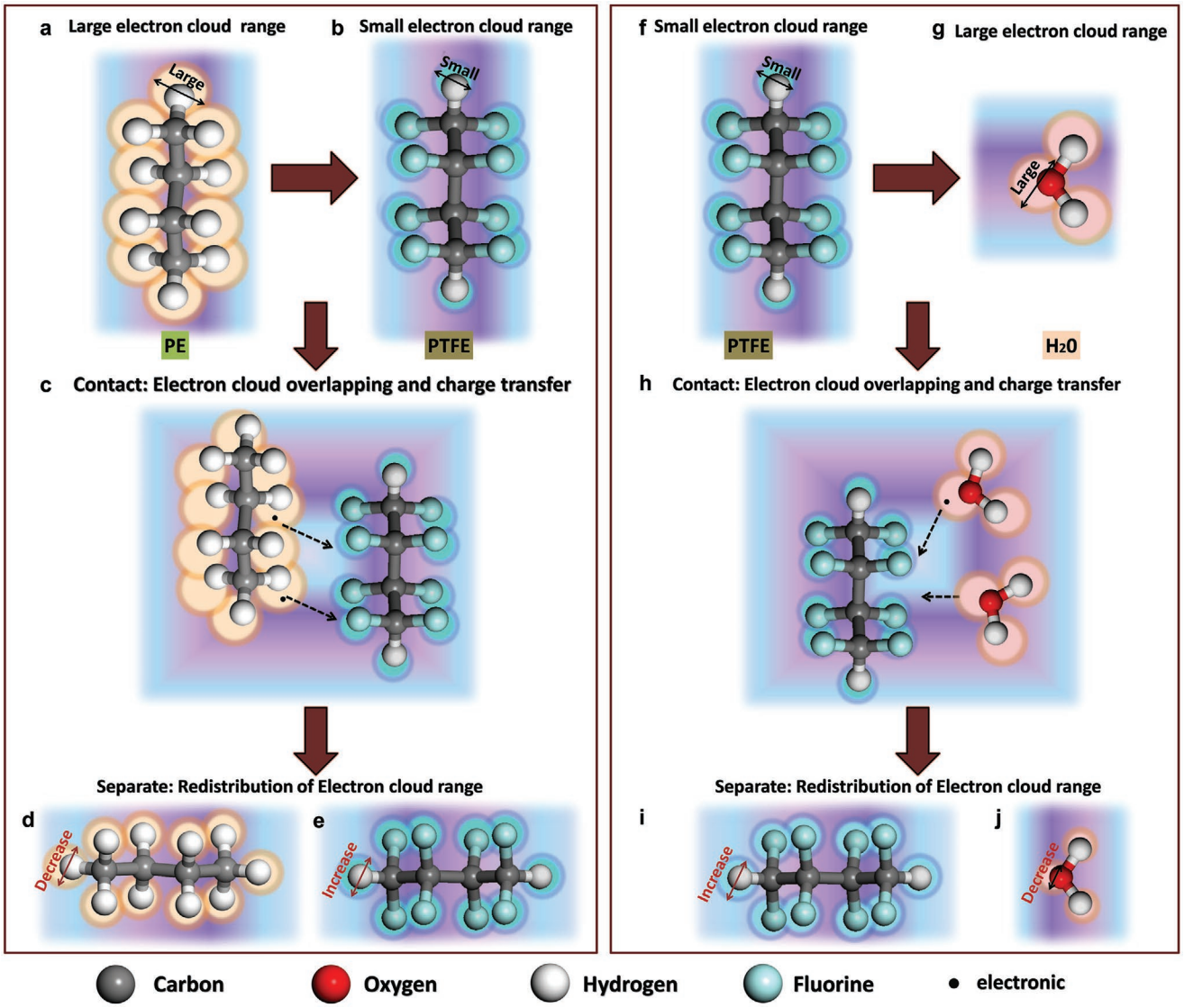

Figure 4. In the case of the main chain is same, the electron cloud range of different groups in the side chain is shown here. Polymer–polymer mode: a) PE film has high electron cloud range with light orange color. b) PTFE film has low electron cloud range with bright blue color. c) When the two films are in contact, their electron clouds partially overlap, and the electrons move from the PE film to the PTFE film. The two films are separated: d) the electron cloud of PE decreases; e) the electron cloud of PTFE increases. Polymer–liquid mode: f) PTFE film has small electron cloud range with bright blue color. g) H_2O has large electron cloud range with light red color. h) During the contact, their electron clouds partially overlap, and electron transfer happens. When they are separated: i) the electron cloud of the H_2O becomes smaller; j) the electron cloud of the PTFE becomes larger, the whole system reaches equilibrium.

the molecular chain of the entire polymer in Figure 4. In the polymer–polymer (PE and PTFE) mode (Figure 4a–e), the electron cloud of H atom in PE film is expressed as a light orange (Figure 4a) and the electron cloud of F atom in PTFE film is light yellow (Figure 4b). The environment for C in PE film and PTFE film are both $sp^{[3]}$ hybrids, so the dominating atoms for electrification are related to H and F atoms. During the contact, the overlapping of electron cloud allows the electrons to transfer from an atom with low electronegativity to an atom with high electronegativity (the attraction force from the F nuclear is higher), as shown in Figure 4c. Then, the electron cloud range of PE molecule decreases and that of PTFE molecule increases due to electron transfer (Figure 4d,e), prompting the two molecule to reach equilibrium. The separation of two materials allows the transferred charges to stay at one molecule and the CE effect can be achieved. Here, we assume that the transferred electron is shared by the electron cloud of the whole functional group after the separation and thus, the electron cloud distribution of the whole molecular section is changed after electron transfer (Figure 4d,e). As for the polymer–liquid mode (Figure 4f–j), the electron cloud of F atom in PTFE covers a small range (Figure 4f) and the electron cloud of O atom in water molecule occupies a larger range (Figure 4g). During the CE process, as shown in Figure 4h, the electron clouds partially overlap and the electrons in the water may transfer to PTFE film. The electron cloud of PTFE and water molecule

reaches an equilibrium state due to electron transfer. Then, the transferred charges stay at new positions after separation (Figure 4I,j). The bonding force between water molecules is just van der Waals force and thus, the charge recombination effect during the separation is more serious in comparison with polymer–polymer mode. The overlapping of the electron cloud between the twisted molecule chains is only a small probability event. Moreover, if two overlapped electron clouds with comparable EW ability, the electron transfer cannot happen either. This can explain why there are only a small amount of charge is generated during the CE with a large contact area. Hence, by increasing the density of EW groups on the main chain of polymer, we can increase the probability of electron transfer, which can explain the high charge density obtained from PTFE and FEP films.

In the above experiments, we only considered the saturated functional groups of the polymer molecular chain to the CE effect and the effect of unsaturated group on the CE should also be considered. It is important to note that a large number of unsaturated groups can be generated on the surface of the polymer film during the fabrication process. There have been a lot of researches analyzing molecular structure of fluorinated polymer, including both saturated and unsaturated groups at on the polymer chain.[41] However, the influences of these unsaturated groups on the CE effect have not been considered. Taking PTFE as an example, the unsaturated groups with C=C double bond can be generated either on the main chain (−CF=CF−) or at the end of the chain (–$CF=CF_2$). In this work, we have found that magnetron sputtering method can be used to increase the unsaturated groups of the PTFE polymer. A new layer of PTFE film is sputtered on the original PTFE film (treated PTFE) by magnetron sputtering (**Figure 5**a) and the unsaturated groups can be generated at two kinds of positions, as can be seen in Figure 5b,c (main chain and end chain). The morphology of treated and common PTFE film is shown in Figure S10a,d in the Supporting Information, where the roughness of treated PTFE film is ±20 nm and that of untreated PTFE film is ±50 nm (Figure S10b,e, Supporting

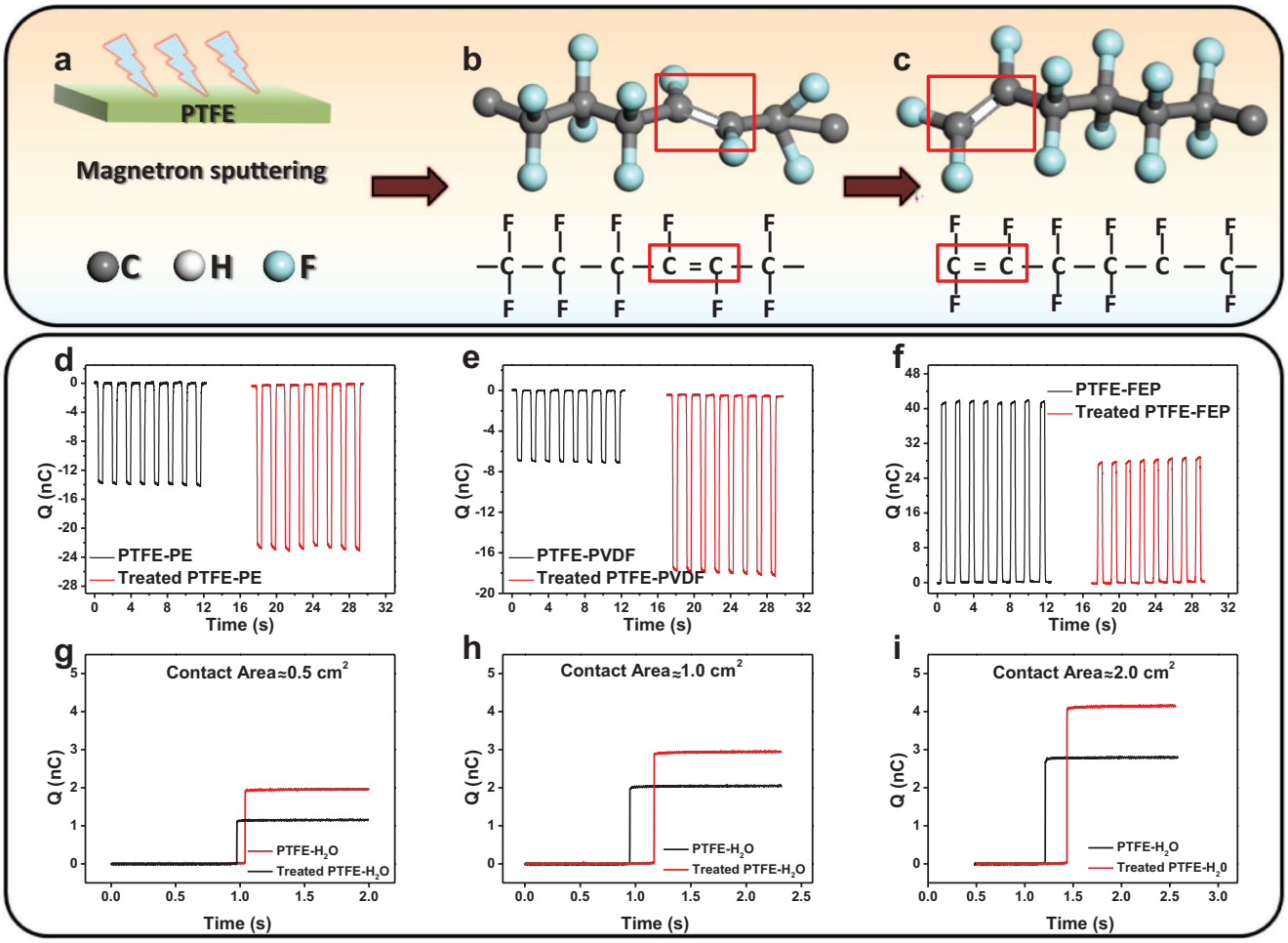

Figure 5. a) Schematic of magnetron sputtered PTFE: the new PTFE is deposited on the original PTFE film by magnetron sputtering (treated PTFE film). The thickness of deposition is about 200 nm. b) A kind of treated PTFE molecular mode with unsaturated groups marked in red boxes. c) Another kind of treated PTFE molecular mode with unsaturated-end groups marked in red boxes. The charge transfer amount (Q) for the original PTFE and the treated PTFE with: d) PE film, as the positive electrode; e) PVDF film, as the positive electrode; f) FEP film, as the negative electrode. The Q for the original/treated PTFE with H_2O in CE, and H_2O as the positive electrode: g) the contact area is about 0.5 cm^2; h) the contact area is about 1.0 cm^2; i) the contact area is about 2.0 cm^2.

Information). In addition, the C/F ratio measured by EDX data increase slightly from 1: 1.886 to 1: 1.969 (Figure S10c,f, Supporting Information). As for the treated PTFE film, the contact angle with water is almost unchanged (Figure S10g,j, Supporting Information). The ATR-FTIR spectrum and XPS spectrum of the treated PTFE and original PTFE can be seen in Figure S10h–l, respectively. In ATR-FTIR spectrum shown in Figure 5b,c, two new peaks can be observed at around 1670–1907 cm^{-1} for the treated PTFE film, which is related to the unsaturated group on the main chain (1723.51 cm^{-1}) and at the end part (1850.11 cm^{-1}).[42] The ATR-FTIR results in Figure S10h,k in the Supporting Information also confirm that the molecular structure of PTFE film before magnetron sputtering mainly has saturated groups, while no increase in the peak signal of the saturated group at 1140.33 or 1201.85 cm^{-1} can be observed after magnetron sputtering. The C atom in the unsaturated group of PTFE molecular chain changes from $sp^{[3]}$ hybrid to $sp^{[2]}$ hybrid orbital. The greater proportion of s orbits in hybrid orbital ($sp,^{[2]}$ 1/3 and $sp,^{[3]}$ 1/4) leads to the stronger ability to attract electrons, which means $sp^{[2]}$ hybrid can provide a stronger EW ability. Accordingly, the existence of C=C double bonds can enhance the EW ability of the whole unsaturated functional group. The XPS results of the two films (Figure S10i,l, Supporting Information) show that the treated PTFE molecule has much more CF_2 bonds than CF_3 bonds, which means the CF_3 on the side chain has been cleared. The treated PTFE surface has the a lot of CF bonds, suggesting the appearance of unsaturated groups on the molecular chain. The unsaturated groups can enhance the film's electrification performance, which can be explained by the electron cloud model. The existence of the C=C double bond decreases the electron cloud range of the whole unsaturated groups and increases the possibility of electron cloud overlapping. For the CE with polymer–polymer mode (the contact area is 40×40 mm), the treated PTFE film with unsaturated groups is significantly more negative than the original PTFE film. The charge transfer amounts of the combination of PE-(treated PTFE) and PVDF-(treated PTFE) increase significantly in comparison with that of original PTFE and the charge transfer amount of (treated PTFE)-FEP decreases (Figure 5d–f) (both PE/PVDF films act as the positive side and FEP film act as the negative side). For the CE with polymer–liquid mode, when the maximum contact area between treated PTFE film and water is about 0.5 cm^2, the charge of CE is 1.9 nC, which is 72% larger than the 1.1 nC of original PTFE film (Figure 5g). When the contact area is increased to be 1, 2, or 4 cm^2 the amount of charge transfer between treated PTFE film and water is still significantly larger than that of PTFE film (Figure 5h,i). Under different contact areas with liquids, the transferred charges of PTFE and treated PTFE film are shown in Figures S11 and S12 in the Supporting Information. The short-circuit current and the matching resistance in the TENG device with PE/treated-PTFE and PE/PTFE can be seen in Figure S13 in the Supporting Information. The stability of the surface charges on the treated-PTFE and PTFE film has also been studied (contact with PE), as can be seen in Figure S14 in the Supporting Information. Currently, PTFE is the most commonly used materials for polymer–liquid energy harvesting, which is probably due to its low cost (cheaper than FEP), excellent stability and large quantities.[3,44–46] Hence, this sputtering method can be a facile and effective method to enhance the performance of solid–liquid type TENG. We have also tried to apply the similar magnetron sputtering treatment for another polymer (PE). The ATR-FTIR results of the PE film before and after sputtering treatment can be seen in Figure S15 in the Supporting Information. The ATR-FTIR spectra of treated PE film shows new peaks at positions of 959.81 and 771.41 cm^{-1} (Figure S15a,b, Supporting Information),[43] which are related to the unsaturated groups on the molecular chain. The electrification performance of sputtering treated PE is tested with PP and PVDF in solid–solid mode (Figure S15c,d, Supporting Information). The output signal from PP-PE combination is enhance, while that from PE-PVDF combination is suppressed. The results from solid–liquid mode of treated PE also show slight enhancement (Figure S15e,f, Supporting Information). Hence, the EW ability of treated PE film is slightly enhanced by sputtering treatment. However, the change of the performance is not so significant in comparison with that of PTFE, which is probably due to the weak EW ability of hydrogen atom in PE. This result confirms that unsaturated groups of the polymer can be increased by the magnetron sputtering, while the performance of CE is highly dominated by the detailed EW ability of functional groups.

In this work, we have studied the contribution of functional groups on polymer chain to the CE effect of both polymer–polymer and polymer–liquid. The F group show the strongest EW ability in comparison with other materials and the increase of the density of F groups on the main chain leads to the increase of charge density, which decides that FEP film with the $-CF_3$ group can offer the highest surface charge density. The similar rules can also be applied for CE of polymer–liquid mode. The polymers with strong EW ability (PTFE and FEP) can generate significant electron transfer effect during the CE with liquids. Nevertheless, for the polymer with quite weak EW ability (PP, PE and PVC), the induced charge amounts are almost unchanged with the increase of contact area, suggesting that the electron transfer effect is quite weak and ion absorption effect may dominate the polymer–liquid CE of these polymers.

More importantly, we have discovered that the unsaturated groups ($-CF=CF_2$ or $-CF=CF-$) of PTFE have much stronger EW ability than the common $-CF_2$ group on the main chain, since the C=C bond in these unsaturated groups can enhance the electronegativity of the whole functional group. The density of these unsaturated groups can be deliberately increased by sputtering a thin film of PTFE on the original surface of PTFE film, indicating a facile and effective way to enhance the performance of a TENG device. In addition, the study of unsaturated groups may also offer some different explanations to other surface modification methods of TENGs such as UV–ozone treatment, inductively coupled plasma etching, and so on. Based on the electron cloud of the atom and the molecular structure of the polymer, we proposed a theoretical mechanism to explain the electron transfer principle between polymer–polymer and polymer–liquid. Hence, a better understanding of the CE on both polymer–polymer and polymer–liquid interfaces can be achieved with the consideration of both electron cloud overlapping and EW ability of functional groups.

Experimental Section

Materials: 7 polymer films, which included PP, PVA, PVC, PE, PVDF, PTFE, FEP were available in the market without further modification. Before the measurements, the polymer films were placed in a vacuum drying oven, heated to 80 °C at 5 °C per minute, then held for an hour for removing all the residual charges. Finally, it was naturally cooled to room temperature to obtain the prepared films. The water used in the experiment was deionized water to remove static electricity. For the polymer–liquid measurements, the experimental details of polymer–liquid measurements, including the parameters for squeezing motion and so on, can be found in the references.[22] The purpose of using the squeezing system was to maximize the contact area between droplet and PTFE and to maximize the amount of transferred charge between water and PTFE. Therefore, the contact time of the liquid with PTFE was within 2 s.

Methods: The electrical signals of all materials were determined by a Keithley 6514 System Electrometer. The separation distance and the motion frequency of TENG were unchanged during all the experiments due to a digital linear motor. Microscopic morphology of the material was given using a scanning SU8020 cold-field scanning electron microscope (SEM), while the elemental analysis was given by energy-dispersive X-ray spectroscopy (EDX) of the SU8020 microscope. The structure of the material was given by a Fourier transform infrared (see FTIR, VERTEX80v) spectrophotometer in attenuated total reflectance mode (ATR) with the pristine and selected polymers was scanned from 4000 to 500 cm^{-1}. The X-ray photoelectron spectroscopy (XPS) investigation was measured by a VG ESCALAB MKII spectrometer with an Mg Kα excitation (1253.6 eV). The roughness and the contact angle of the material were given by a step meter (KLA-TencorP7) and a contact angle measuring machine (CA100C), respectively. PTFE film with unsaturated double bonds was prepared by a Denton magnetron sputtering coating instrument (Discovery635).

Supporting Information

Supporting Information is available from the Wiley Online Library or from the author.

Acknowledgements

S.L. and J.N. contributed equally to this work. This work was supported by the National Key R&D Project from Minister of Science and Technology (2016YFA0202704), the National Natural Science Foundation of China (Grant No. 51775049), Beijing Natural Science Foundation (4192069), the Beijing Municipal Science & Technology Commission (Z171100000317001), and Young Top-Notch Talents Program of Beijing Excellent Talents Funding (2017000021223ZK03).

Conflict of Interest

The authors declare no conflict of interest.

Keywords

molecular chains, polymer electrification, triboelectric nanogenerators, unsaturated function groups

Received: February 25, 2020
Revised: April 4, 2020
Published online:

[1] Z. L. Wang, A. C. Wang, *Mater. Today* **2019**, *30*, 34.
[2] H. T. Baytekin, A. Z. Patashinski, M. Branicki, B. Baytekin, S. Soh, B. A. Grzybowski, *Science* **2011**, *333*, 308.
[3] W. Xu, H. Zheng, Y. Liu, X. Zhou, C. Zhang, Y. Song, X. Deng, M. Leung, Z. Yang, R. X. Xu, Z. L. Wang, X. C. Zeng, Z. Wang, *Nature* **2020**, *578*, 392.
[4] R. Williams, J. Coll, *Interface Sci.* **1982**, *88*, 530.
[5] Y. Sun, X. Huang, S. Soh, *Angew. Chem.* **2016**, *55*, 9956.
[6] L. S. McCarty, G. M. Whitesides, *Angew. Chem., Int. Ed.* **2008**, *47*, 2188.
[7] J. Nie, Z. Wang, Z. Ren, S. Li, X. Chen, Z. L. Wang, *Nat. Commun.* **2019**, *10*, 2264.
[8] Z. H. Lin, G. Zhu, Y. S. Zhou, Y. Yang, P. Bai, J. Chen, Z. L. Wang, *Angew. Chem., Int. Ed.* **2013**, *52*, 5065.
[9] T. J. Lewis, *J. Phys. D: Appl. Phys.* **1990**, *23*, 1469.
[10] L. Huang, S. Lin, Z. Xu, H. Zhou, J. Duan, B. Hu, J. Zhou, *Adv. Mater.* **2020**, *32*, 1902034.
[11] H. Chang, G. Wang, A. Yang, X. Tao, X. Liu, Y. Shen, Z. A. Zheng, *Adv. Funct. Mater.* **2010**, *20*, 2893.
[12] K. Parida, G. Thangavel, G. Cai, X. Zhou, S. Park, J. Xiong, P. S. Lee, *Nat. Commun.* **2019**, *10*, 2158.
[13] Z. L. Wang, W. Wu, *Angew. Chem., Int. Ed.* **2012**, *51*, 11700.
[14] G. G. Touchard, T. W. Patzek, C. J. Radke, *IEEE Trans. Ind. Appl.* **1996**, *32*, 1051.
[15] L. E. Helseth, X. D. Guo, *Langmuir* **2015**, *31*, 3269.
[16] D. Choi, D. S. Kim, *Langmuir* **2014**, *30*, 6644.
[17] D. Yoo, S.-C. Park, S. Lee, J.-Y. Sim, I. Song, D. Choi, H. Lim, D. S. Kim, *Nano Energy* **2019**, *57*, 424.
[18] D. Choi, D. Yoo, K. J. Cha, M. La, D. S. Kim, *Nano Energy* **2017**, *36*, 250.
[19] C. Xu, A. C. Wang, H. Zou, Y. Dai X. He, P. Wang, Y. Wang, P. Feng, D. Li, Z. L. Wang, *Adv. Mater.* **2018**, *30*, 1706790.
[20] S. Lin, L. Xu, L. Zhu, X. Chen, Z. L. Wang, *Adv. Mater.* **2019**, *31*, 1901418.
[21] S. Lin, L. Xu, C. Xu, Z. L. Wang, *Adv. Funct. Mater.* **2020**, *30*, 1909724.
[22] J. Nie, Z. Ren, L. Xu, S. Lin, F. Zhan, X. Chen, Z. L. Wang, *Adv. Mater.* **2020**, *32*, 1905696.
[23] S. Lin, L. Xu, A. C. Wang, Z. L. Wang, *Nat. Commun.* **2020**, *11*, 399.
[24] P. K. Yang, L. Lin, F. Yi, X. Li. K. C. Pradel, Y. Zi, C. Wu, J. H. He, Y. Zhang, Z. L. Wang, *Adv. Mater.* **2015**, *27*, 3817.
[25] V. K. Thakur, G. Ding, J. Ma, P. S. Lee, X. Lu, *Adv. Mater.* **2012**, *24*, 4071.
[26] Y. Qian, J. Nie, X. Ma, Z. Ren, J. Tian, J. Chen, H. Shen, X. Chen, Y. Li, *Nano Energy* **2019**, *60*, 493.
[27] Y. Ding, Y. Shi, J. Nie, Z. Ren, S. Li, F. Wang, J. Tian, X. Chen, Z. L. Wang, *Chem. Eng. J.* **2020**, *388*, 124369.
[28] X. Ma, S. Li, M. Iwamoto, S. Lin, L. Zheng, X. Chen, *Nano Energy* **2019**, *66*, 104090.
[29] S. H. Shin, Y. H. Kwon, Y. H. Kim, J. Y. Jung, M. H. Lee, J. Nah, *ACS Nano* **2015**, *9*, 4621.
[30] J. W. Lee, H. J. Cho, J. S. Chun, K. N. Kim, S. Kim, C. W. Ahn, I. W. Kim, J.-Y. Kim, S.-W. Kim, C. Yang, J. M. Baik, *Sci. Adv.* **2017**, *3*, 1602902.
[31] J. P. Lee, J. W. Lee, J. M. Baik, *Micromachines* **2018**, *9*, 532.
[32] S. Li, Y. Fan, H. Chen, J. Nie, Y. Liang, X. Tao, J. Zhang, X. Chen, E. Fu, Z. L. Wang, *Energy Environ. Sci.* **2020**, *13*, 896.
[33] P. K. Yang, Z. H. Lin, K. C. Pradel, L. Lin, X. Li, X. Wen, H. J. He, Z. L. Wang, *ACS Nano* **2015**, *9*, 901.
[34] A. C. Wang, B. Zhang, C. Xu, H. Zou, Z. Lin, Z. L. Wang, *Adv. Funct. Mater.* **2020**, 1909384.
[35] J. K. Moon, J. Jeong, D. Lee, H. K. Pak, *Nat. Commun.* **2013**, *4*, 1487.
[36] L. E. Helseth, *Langmuir* **2019**, *35*, 8268.
[37] R. Zimmermann, S. Dukhin, C. Werner, *J. Phys. Chem. B* **2001**, *105*, 8544.

[38] J. K. Beattie, A. M. Djerdjev, *Angew. Chem., Int. Ed.* **2004**, *43*, 3568.
[39] J. K. Beattie, A. M. Djerdjev, G. V. Franks, G. G. Warr, *J. Phys. Chem. B* **2005**, *109*, 15675.
[40] D. C. Taflin, T. L. Ward, E. J. Davis, *Langmuir* **1989**, *5*, 376.
[41] M. I. Bro, C. A. Sperati, *J. Polym. Sci.* **1959**, *38*, 289.
[42] M. Pianca, E. Barchiesi, G. Esposto, S. Radice, *J. Fluor. Chem.* **1999**, *95*, 71.
[43] R. J. de Kock, P. A. H. M. Hol, *Polym. Lett.* **1964**, *2*, 339.
[44] F. Yi, L. Lin, S. Niu, P. K. Yang, Z. Wang, J. Chen, Y. Zhou, Y. Zi, J. Wang, Q. Liao, Y. Zhang, Z. L. Wang, *Adv. Funct. Mater.* **2014**, *24*, 7488.
[45] M. Wang, J. Zhang, Y. Tang, J. Li, B. Zhang, E. Liang, Y. Mao, X. Wang, *ACS Nano* **2018**, *12*, 6156.
[46] J. H. Lee, S. M. Kim, T. Y. Kim, U. Khan, S. W. Kim, *Nano Energy* **2019**, *58*, 579.